HHS Public Access

Author manuscript

Circulation. Author manuscript; available in PMC 2020 May 14.

Published in final edited form as:

Circulation. 2019 May 14; 139(20): 2342–2357. doi:10.1161/CIRCULATIONAHA.117.028752.

Fibroblast Primary Cilia are Required for Cardiac Fibrosis

Elisa Villalobos, PhD[1,3,†], **Alfredo Criollo, PhD**[1,3,4,†], **Gabriele G. Schiattarella, MD, PhD**[1], **Francisco Altamirano, PhD**[1], **Kristin M. French, PhD**[1], **Herman I. May, MSc**[1], **Nan Jiang, MSc**[1], **Ngoc Uyen Nhi Nguyen, PhD**[1], **Diego Romero, MSc**[5], **Juan Carlos Roa, MD**[5], **Lorena García, PhD**[3], **Guillermo Diaz-Araya, PhD**[3], **Eugenia Morselli, PhD**[6], **Anwarul Ferdous, PhD**[1], **Simon J. Conway, PhD**[7], **Hesham A. Sadek, MD, PhD**[1], **Thomas G. Gillette, PhD**[1], **Sergio Lavandero, PhD**[1,3,*], and **Joseph A. Hill, MD, PhD**[1,2,*]

[1]Department of Internal Medicine (Cardiology), University of Texas Southwestern Medical Center, Dallas, TX 75390-8573, USA

[2]Department of Molecular Biology, University of Texas Southwestern Medical Center, Dallas, TX 75390-8573, USA

[3]Advanced Center for Chronic Diseases (ACCDiS), Faculty of Chemical Pharmaceutical Sciences & Faculty of Medicine, University of Chile, Santiago 8380492, Chile,

[4]Research Institute for Odontology Sciences, Faculty of Odontology, University of Chile, Santiago 8380492, Chile,

[5]Department of Pathology, Faculty of Medicine, Pontifical Catholic University of Chile, Santiago 7820436, Chile

[6]Department of Physiology, Faculty of Biological Sciences, Pontifical Catholic University of Chile, Santiago 7820436, Chile

[7]Wells Center for Pediatric Research, Indiana University School of Medicine, Indianapolis, IN 46202-3082 USA.

Abstract

BACKGROUND: The primary cilium is a singular cellular structure that extends from the surface of many cell types and plays crucial roles in vertebrate development, including that of the heart. Whereas ciliated cells have been described in developing heart, a role for primary cilia in adult heart has not been reported. This, coupled with the fact that mutations in genes coding for multiple ciliary proteins underlie polycystic kidney disease, a disorder with numerous cardiovascular manifestations, prompted us to identify cells in adult heart harboring a primary cilium and to determine whether primary cilia play a role in disease-related remodeling.

Correspondence: Joseph A. Hill, MD, PhD, Department of Internal Medicine (Cardiology) University of Texas Southwestern Medical Center. 6000 Harry Hines Blvd, Dallas, Texas, 75390-8573, USA. Joseph.Hill@UTSouthwestern.edu, or, Sergio Lavandero, PhD, Advanced Center for Chronic Diseases (ACCDiS), Faculty Chemical & Pharmaceutical Sciences, University of Chile. Olivos 1007, Santiago 8380492, Chile. slavander@uchile.cl.

† Co-first authors;

* Co-senior authors

DISCLOSURES

None.

METHODS: Histological analysis of cardiac tissues from C57BL/6 mouse embryos, neonatal, and adult mice was performed to evaluate for primary cilia. Three injury models (apical resection, ischemia/reperfusion and myocardial infarction) were employed to identify the location and cell type of ciliated cells using antibodies specific for cilia (acetylated tubulin, γ-tubulin, PC1, PC2, and KIF3A), fibroblasts (vimentin, α-smooth muscle actin, and fibroblast-specific protein-1) and cardiomyocytes (α-actinin and troponin I). A similar approach was used to assess for primary cilia in infarcted human myocardial tissue. We studied mice silenced exclusively in myofibroblasts for PC1 and evaluated the role of PC1 in fibrogenesis in adult rat fibroblasts and myofibroblasts.

RESULTS: We identified primary cilia in mouse, rat, and human heart, specifically and exclusively in cardiac fibroblasts. Ciliated fibroblasts are enriched in areas of myocardial injury. Transforming growth factor beta-1 (TGF-β1) signaling and SMAD3 activation were impaired in fibroblasts depleted of the primary cilium. Extracellular matrix protein levels and contractile function were also impaired. *In vivo*, depletion of PC1 in activated fibroblasts after myocardial infarction impaired the remodeling response.

CONCLUSIONS: Cardiac fibroblasts in the neonatal and adult heart harbor a primary cilium. This organelle and its requisite signaling protein, PC1, are required for critical elements of fibrogenesis, including TGF-β1-SMAD3 activation, production of extracellular matrix proteins, and cell contractility. Together, these findings point to a pivotal role of this organelle, and PC1, in disease-related pathological cardiac remodeling, and suggest that some of the cardiovascular manifestations of autosomal dominant polycystic kidney disease derive directly from myocardium-autonomous abnormalities.

Journal Subject Terms:

Basic Science Research; Translational Studies; Cardiac Disease

Keywords

PC1; fibrogenesis; cardiac fibroblast; polycystin-1; TGF-1

INTRODUCTION

The primary cilium is a cellular organelle formed by a protrusion of the plasma membrane that functions as a signaling platform in eukaryotic cells.[1] The organelle is found in many quiescent cells, including neurons, preadipocytes, and kidney tubule cells,[2–4] where it has been reported to be involved in a variety of cellular functions such as proliferation, differentiation, and cell cycle regulation.[5, 6] These functions also include mechanochemical sensing of diverse stimuli, including growth factors[7], leptin[8], glucocorticoids[9], amino acids[10] and mechanical stress.[11] The structure comprises microtubular projections at the cilia axoneme that are stabilized by acetylation of structural tubulin molecules.

The importance of cilia is highlighted by their role in several diseases known as ciliopathies, such as Bardet–Biedl syndrome and polycystic kidney disease.[12] Within these disorders, the most relevant genetic mutants occur in *Pkd1* (coding for polycystin-1, PC1), *Pkd2* (coding for polycystin-2, PC2), *Kif3A* (coding for kinesin family member 3A) and *Ift88* (coding for

intraflagellar transport 88) genes.[1, 13, 14] These mutations culminate in alterations in cilia assembly (Kif3A, Ift88) or function (*Pkd1*, *Pkd2*).[15] Downregulation of the primary cilium and PC1 are associated with alterations in extracellular matrix (ECM) proteins[13] and in aortic valve development.[16] Furthermore, increased numbers of ciliated cells are seen in lung tissue from patients with idiopathic pulmonary fibrosis.[17]

In the heart, the presence of primary cilia and associated function are poorly characterized. Using electron microscopy in 1969, Rash *et al.* first reported the presence of primary cilia in embryonic and adult heart in several species.[18] In analyses of chick heart development, cilia were observed in differentiating myoblasts, myocytes, fibroblasts and fibrocytes.[18] Subsequent studies described cardiac primary cilia in embryonic and adult human heart[14, 19] and in aortic endothelial cells.[20] However, it remains unclear which cardiac cell types express cilia and whether this organelle participates in cardiovascular physiology or disease.

METHODS

All supporting data are available within the article. Detailed materials and methods are described in the Online Data Supplement.

Human Samples

Samples were obtained from Pontificia Universidad Catolica de Chile Biobank (Santiago). The donors gave written informed consent. The study was approved by the institutional review board and for the Institutional Ethics Committee of the Pontificia Universidad Catolica de Chile. Details regarding the patients are provided (Online Data Supplement Table 1).

Animal studies

Mouse and rat protocols and procedures were approved by the Institutional Animal Care and Use Committee of the University of Texas Southwestern Medical Center IACUC and the University of Chile.

Quantitative RT-PCR Assay

Primer sequences used for Quantitative RT-PCR Assay are provided (Online Data Supplement Table 2). All primers were previously calibrated and used at efficiencies between 90–110%.

Statistical Analysis

Data are presented as mean ± SEM of multiple independent experiments/animals. Data were analyzed either by the Student unpaired *t* test to compare means when there were two experimental groups, by one-way ANOVA followed by Dunnett's *post-hoc* test to compare means among ≥ 3 groups, or by two-way ANOVA to compare means when there were two or more independent variables. Data were analyzed statistically with GraphPad Prism 7.04 (for Windows). Differences were considered significant at $p < 0.05$.

RESULTS

Primary cilia are present in mouse heart

To test for the presence of ciliated cells in neonatal and adult mouse heart, we examined tissue sections from 1- and 10-week-old male C57BL/6 mice. We identified cilia in both neonatal and adult mouse hearts (Figures 1A, 1B), as evidenced by staining for acetylated tubulin, a protein enriched along the primary cilium.[21, 22] Cilia have been implicated in a wide range of functions during development in mice.[4, 23] In this regard, we evaluated whether cilia can be detected at different stages of heart development (E9.5, E10.5, E11.5, E12.5 and E15.5) (Figure 1C). We identified cilia in hearts at embryonic stages E10.5, E11.5, E15.5 (Figure 1D, Online Data Supplement Figure S1A–S1B). Furthermore, we uncovered that these ciliated cells do not correspond to cardiomyocytes, as they did not stain for the cardiomyocyte-specific protein troponin I (Figures 1C, 1D, Online Data Supplement Figure S1A–S1B).

To confirm the absence of primary cilia in adult cardiomyocytes, we depleted cells of KIF3A, a protein required for primary cilium morphogenesis.[24, 25] We studied heart tissues isolated from wild-type, *Kif3a*$^{F/F}$, and cardiomyocyte-specific KIF3A KO mice (*αMhc-cre;Kif3a*$^{F/F}$). Interestingly, these efforts revealed the presence of ciliated cells in *Kif3a*$^{F/F}$ and *αMhc-cre;Kif3a*$^{F/F}$ mice (Online Data Supplement Figure S1C–S1D). Given that KIF3A is a protein fundamental to cilia assembly[24, 26], our results confirm that ciliated cells in embryonic heart do not correspond to cardiomyocytes.

Next, we isolated neonatal and adult rat cardiomyocytes. Cultures were co-stained for α-actinin (cardiomyocyte marker) and acetylated tubulin (primary cilium marker). Cardiomyocytes stained positive for α-actinin, and yet no cilia were identified (Online Data Supplement Figures S1E–S1F). Conversely, cilia were readily detected in the pre-adipocyte cell line 3T3-L1, which served as a positive control (Online Data Supplement Figure S1G). We next evaluated levels of acetylated tubulin in cardiomyocytes and cardiac fibroblasts from neonatal and adult rats, observing no significant differences in the protein levels from these two cell types (data not shown). In aggregate, our results confirm the presence of primary cilia in mouse and rat hearts and that cells harboring this organelle are not cardiomyocytes.

Ciliated cells accumulate in heart following injury

After establishing the presence of cells harboring primary cilia in neonatal and adult mouse hearts, we next assessed whether the abundance of ciliated cells is modified following myocardial injury. Adult male C57BL/6 mice were subjected to ischemia for 45 min followed by reperfusion for 4, 7, or 14 days (ischemia/reperfusion, I/R) surgery. Sham surgery was performed as a control (Figure 2A). We observed significant enrichment of ciliated cells in the infarcted zone in adult cardiac tissue. Ciliated cells stained positive for vimentin, suggesting that they are fibroblasts (Figure 2B).

Next, 7 day-old C57BL/6 mice were subjected to apical resection, a model characterized by development of fibrosis in the injured zone.[27] Seven days post-surgery, hearts were collected and processed to evaluate for cilia (Figure 2C). Interestingly, we found that the abundance of

ciliated cells increased in the zone of pathological injury. As before, the ciliated cells were not cardiomyocytes, as they did not stain positive for troponin I (Figure 2C).

To test for the presence of cilia in other cell types, we probed for acetylated tubulin in hearts of adult male C56BL/6 mice 7 days following myocardial infarction (MI) surgery. We co-stained cardiac tissue with markers specific for myofibroblasts (α-smooth muscle actin, α-SMA), macrophages (cluster of differentiation 68, CD68) and endothelial cells (platelet/endothelial cell adhesion molecule-1, PECAM1 or CD31). These experiments revealed that the ciliated cells largely co-stain for α-SMA (Figure 2D–2G). To confirm these results, we tested *in vitro* for the presence of cilia in cultures of adult rat ventricular myocytes (ARVM), neonatal rat ventricular myocytes (NRVM), adult rat cardiac fibroblasts (ARCF), a murine macrophage cell line (RAW 264.7), human umbilical vein endothelial cells (HUVEC), and human aortic endothelial cells (HAEC). Interestingly, the characteristic antenna-like shape of primary cilia was observed exclusively in cardiac fibroblasts (Online Data Supplement Figure S1E–S1F and Figure S2). Altogether, we identified primary cilia localized exclusively to fibroblasts and accumulated in areas of myocardial injury.

Thus, our results confirmed the presence of primary cilia in mouse heart. However, their presence in human cardiac tissue remains unclear. Therefore, we set out to evaluate the presence of primary cilia in human myocardial tissue obtained from 6 patients at the time of cardiac transplantation surgery. Masson's trichrome staining revealed strong collagen deposition, indicative of myocardial fibrosis and scar tissue (Figure 2H). Immunofluorescence analysis, positive for vimentin and fibroblast specific protein 1 (FSP-1), pointed to these cells being fibroblasts (Figure 2I and Online Data Supplement Figure S3A). Thus, our findings revealed – again – that cardiac fibroblasts, in this case human, harbor primary cilia.

Primary cilia are present in rat cardiac fibroblasts

Given our findings that cardiac fibroblasts in mouse and human heart harbor a primary cilium, we tested for their presence in rat cardiac fibroblasts. To do this, we prepared primary cultures of neonatal and adult rat cardiac fibroblasts (NRCF and ARCF, respectively) and tested for the presence of primary cilia. To accomplish this, we immunostained for acetylated tubulin, a marker of the ciliary tail[21] and γ-tubulin, a marker of the cilia base.[22] Probing for vimentin was used to confirm that the identified cells were fibroblasts. Under basal conditions, 49.9% (± 24.4, n=10) of the ARCF harbored a primary cilium, and this number increased to 72.5% (± 11.0, n=8, $p<0.05$) after TGF-β1 (transforming growth factor beta-1) treatment (data not shown). These studies revealed that both NRCF and ARCF harbor primary cilia (Figures 3A, 3B), consistent with our findings in myocardial tissue (Figure 2).

To begin to test for a functional role of these organelles, we investigated whether PC1 and PC2 proteins, implicated in cilia-dependent signaling events, are localized to the primary cilium in cardiac fibroblasts. We found that not only PC1 and PC2, but also KIF3A, a key protein required for cilia biogenesis and function[5, 11] are present in the primary cilium of NRCF (Figure 3C).

Cilia and PC1 are required for TGF-β1-induced fibrosis

Previously, TGF-β1 receptors were identified in the pocket region of primary cilia from human foreskin fibroblasts, and they were reported to participate in TGF-β1-mediated SMAD2/3 phosphorylation.[28] Given our detection of primary cilia in cardiac fibroblasts, we set out to determine whether these organelles participate in fibrogenesis, a major function of these cells. Recognizing that TGF-β1, through both autocrine and paracrine mechanisms, triggers a fibrogenic response in cultured cardiac fibroblasts, acting via the SMAD2/3/4 axis[29], we silenced fibroblasts of key functional and structural ciliary proteins. Specific siRNA-mediated silencing of PC1, PC2, or KIF3A was performed in NRCF (Online Data Supplement Figure S4A–S4C and Figure 4A), and cells were subsequently treated with TGF-β1 (48 h). Our data reveal that the structural ciliary proteins KIF3A and PC1 are required for TGF-β1-induced collagen type I biosynthesis (Figures 4A, 4B). Interestingly, knockdown of PC2 did not alter this signaling response.

Next, we performed quantitative PCR assays for fibronectin, collagen type I, and collagen type III in the presence/absence of TGF-β1 in cells depleted of KIF3A or PC1 by specific siRNA. These experiments confirmed our prior findings, demonstrating that KIF3A and PC1 are required for the up-regulation of these ECM proteins (Figure 4E–4G).

We then turned to ARCF to evaluate the role of another ciliary structural protein in the TGF-β1-induced fibrotic response. IFT88 is a protein required for ciliogenesis and cilia function.[4] ARCF were depleted of IFT88 using siRNA (Figure 4H), and, consistent with our findings in NRCF, IFT88 knockdown blunted TGF-β1-induced collagen type I and α-smooth muscle actin (α-SMA) biosynthesis (Figures 4H, 4I). These findings highlight, once again, the relevance of primary cilia in the myocardial fibrogenic response.

A cardinal feature of myofibroblasts is α-SMA expression and consequent contractile activity essential to wound healing.[30, 31] To test for a functional role of primary cilia in fibroblast differentiation into myofibroblasts, we exposed NRCF to TGF-β1 (10 ng/mL, 48 h) and evaluated α-SMA gene expression (Figure 4L) and contractile function (Figures 4J, 4K). Cells that were selectively depleted of PC1 showed no increase in α-SMA transcript levels, and TGF-β1-driven contraction was blunted significantly (Figures 4J, 4L).

Next, we evaluated the relevance of PC1 and primary cilia in other characteristic fibroblast processes, *viz.* cell migration, matrix invasion, and substrate adhesion. A role for PC1 in cell migration and focal adhesion kinase (FAK) phosphorylation at Tyr 397 has been reported in other cell types.[32, 33] To evaluate the influence of PC1 and primary cilia on these processes, we studied ARCF cultures depleted of PC1 and KIF3A using specific siRNAs. After knockdown, we detached the cells from the culture plate with trypsin and allowed them to reattach (overnight) to evaluate the activation of FAK. These experiments were performed in the presence or absence of TGF-β1. Interestingly, we detected no significant difference in TGF-β1-elicited pFAK (Tyr397) after depletion of either PC1 or KIF3A (Online Data Supplement Figure S5A–S5B). Furthermore, we evaluated vinculin distribution and localization by immunofluorescence. Vinculin is an accessory protein present in focal adhesions.[34] We uncovered a perinuclear vinculin distribution in cells depleted of PC1 as compared with control cells (UNR). (Online Data Supplement Figure S5C). Additionally,

we performed migration (2D) and invasion (3D) assays with ARCF following PC1 and KIF3A depletion. We did not observe significant alterations in migration or matrix invasion in cells in which PC1 or KIF3A was depleted (Online Data Supplement Figure S5D–S5G).

Overall, our results demonstrate that cardiac fibroblast primary cilia are functional and participate in TGF-β1-elicited fibrogenesis and myofibroblast differentiation. Moreover, PC1 is involved in the synthesis of ECM proteins and in fibroblast contractile function and yet not involved in fibroblast migration, matrix invasion or focal adhesion activation.

Primary cilia and PC1 are required for TGF-β1-mediated SMAD3 signaling

Given that SMAD proteins are required for TGF-β1-induced fibrosis[35, 36] and that the primary cilium can function as a localized platform for critical signaling pathways[4–6, 8, 12, 37], we evaluated whether structural ciliary proteins regulate TGF-β1-mediated SMAD3 phosphorylation. As expected, TGF-β1 increased the phosphorylation of SMAD3 in both NRCF (Online Data Supplement Figures S4D, S4E) and ARCF (Online Data Supplement Figures S4F–S4G). Importantly, depletion of either KIF3A or PC1 in NRCF significantly attenuated TGF-β1-dependent SMAD3 phosphorylation (Figures 5A, 5B). Evaluation of the subcellular localization of phospho-SMAD3 (p-SMAD3) in ARCF by immunofluorescence revealed increased nuclear staining of p-SMAD3 after exposure to TGF-β1 (30 min) (Figure 5C) and decreased intensity in cells in which KIF3A and PC1 was depleted (Figure 5D).

Altogether, these results lend additional support to a model in which primary cilia and PC1 participate in cardiac fibrogenesis and point to a critical role of this signaling platform in TGF-β1-dependent activation of SMAD3 during fibrosis.

Silencing of PC1 in activated fibroblasts promotes adverse cardiac remodeling following myocardial infarction

Next, we set out to test the contribution of PC1 in cardiac fibrogenesis *in vivo*. To accomplish this, we engineered fibroblast-specific *Pkd1* knockout mice (*Postn-Cre;Pkd1*$^{F/F}$), driving *Cre* recombinase expression with the *periostin* promoter, which is activated after cardiac injury.[38] As expected, *Pkd1* knockout animals did not manifest a phenotype under basal conditions assessed by morphometric or functional parameters (Online Data Supplement Figure S6 and Online Data Supplement Table 3). Then, to activate *Cre* expression, MI surgery was performed in control (*Pkd1*$^{F/F}$) and knockout (*Postn-Cre; Pkd1*$^{F/F}$) mice, and hearts were harvested 7 days post-surgery (Figure 6A). Efficient gene recombination (Online Data Supplement Figure S7A) was confirmed. Next, immunofluorescence analysis of a marker specific for activated fibroblasts (α-SMA) and for the C-terminus of PC1 (PC1-CT) (Figure 6B) demonstrated strong reduction of PC1-CT staining in α-SMA positive cells, suggesting that PC1 was successfully depleted in activated cardiac fibroblasts.

We employed another strategy to validate our model and confirm PC1 depletion in activated fibroblasts. For this purpose, we bred *Postn-Cre; Pkd1*$^{F/F}$ mice with mice expressing Rosa26-TdTomato to generate *Postn-Cre; Pkd1*$^{F/+}$; Rosa26-TdTomato mice. Owing to the presence of a reporter gene, we were able to track gene recombination after MI by the

presence of TdTomato-positive cells. As expected, we detected robust TdTomato fluorescence post-MI due to Cre-mediated recombination with localization occurring largely in the scar area and within cells that are α-SMA positive (activated fibroblasts) (Online Data Supplement Figure S7I).

Interestingly, fibroblast-specific *Pkd1* knockout mice developed an enhanced hypertrophic response post-MI, manifested as heart weight/tibia length (HW/TL) and by cardiomyocyte cross-sectional area (CSA) (Figure 6E, 6H, 6I). Furthermore, MI scar size was decreased significantly in *Pkd1* knockout mice as compared with control mice (26 ± 8% versus 20 ± 6%, respectively, $p<0.05$) (Figure 6C, 6D). Together, these results point to PC1 as playing a novel role in post-MI myocardial remodeling.

Interestingly, survival and echocardiographic parameters did not manifest significant differences between groups (Online Data Supplement Figure S7C, Figure 6G and Online Data Supplement Table 4). Quantification of the fibrosis response, assayed in distinct zones of tissue (remote, border, scar) by Masson's trichrome staining, picrosirius red staining, and under polarized light, did not uncover significant differences between *Pkd1* knockout and control mice (Figure 7A–7D & Online Data Supplement Figure S7E).

After MI, a robust population of activated fibroblasts was detected at the site of the MI scar (Figure 6B, Online Data Supplement Figure S7D & S7I). In light of this, we evaluated mRNA and protein levels of classic fibrosis markers, including fibronectin, collagen I, and α-SMA. Surprisingly, mRNA and protein levels of these markers remained similar across the groups (Online Data Supplement Figure 7F and Figure 7E–7H). However, when we measured levels of soluble collagen from MI scar, we detected significant reductions in *Pkd1* knockout mice (Figure 7I). Overall, these results reveal that PC1 plays a major role in post-MI cardiac remodeling, such that depletion of PC1 in activated cardiac fibroblasts promotes myocardial hypertrophy and triggers alterations in scar architecture.

PC1 is required for myofibroblast contractile activity

Having uncovered a novel role of activated fibroblast PC1 in post-MI cardiac remodeling, we set out to test the relevance of PC1 in myofibroblast function (Figure 8). First, we isolated and differentiated ARCF into myofibroblasts (TGF-β1, 96 h) (Figure 8A). Then, we evaluated mRNA and protein levels of collagen I, fibronectin, and α-SMA in cells treated with siRNA specific for PC1. Efficiency of PC1 knockdown in activated fibroblasts was first confirmed; protein levels diminished to 17.4% ± 0.06 (Figure 8B, 8C). Consistent with our *in vivo* data, we observed no significant differences in transcript and protein levels between the cells depleted of PC1 versus controls (UNR) (Figure 8D–8H).

Next, we tested for functional relevance by evaluating myofibroblast contractile activity, employing a contraction assay performed in floating collagen matrix. Unexpectedly, we detected larger areas of collagen matrix in cells depleted of PC1 levels. Together, these results confirm that PC1 is required for ECM contractile function even though it is not required for the up-regulation of fibrosis markers after myofibroblast commitment (Figure 8I, 8J).

DISCUSSION

In the last decade, several studies have identified the primary cilium as a critical signaling organelle.[10, 12, 25] Although a pioneering study in the 1970's reported that human cardiac samples harbored ciliary structures, specific cell location and function of cilia in the heart has never been clarified.[14] Indeed, a potential role for this organelle in adult heart has never been elucidated. Here, we report that cells harboring a primary cilium exist in developing and adult mouse heart, as well as in adult human myocardium. These cells, however, are not cardiomyocytes but rather cardiac fibroblasts. We go on to demonstrate that these ciliated fibroblasts accumulate at the site of myocardial injury. Moreover, this organelle and PC1 participate in critical signaling functions, including TGF-β1 responsiveness, SMAD activation, extracellular matrix biogenesis, and fibrogenesis. That said, PC1 and primary cilia are not required for fibroblast migration, matrix invasion or focal adhesion activation. Together, these findings point to a novel role of the primary cilium and PC1 in cardiac physiology and disease pathogenesis (Figure 8K).

Primary cilia

The primary cilium, in contrast with motile cilia, is singular and immotile and serves to sense chemical and mechanical stimuli in a wide range of cell types.[2, 11, 25] Discovered in 1898[39], this organelle was largely ignored for decades, attracting interest only recently. Fluid flow, pressure, hormones, metabolites and growth factors can be sensed by primary cilia, and these extracellular cues are transduced to activate a wide range of signaling pathways.[11, 37] Indeed, primary cilia have been documented in different tissues and found to regulate several physiological and pathological processes.[12, 24, 37] Furthermore, dysfunction or structural alterations in primary cilia underlie ciliopathies with associated myocardial phenotypic defects.[40, 41] For example, heart defects are observed in several ciliopathy syndromes[40], and a genetic screen in fetal mice showed that primary cilia and cilia-transduced signaling cues have important roles in the pathogenesis of congenital heart disease.[41] However, elucidation of molecular mechanisms that control these diseases remained to be accomplished.

Primary cilia participate in myocardial fibrogenesis

Cardiac fibrosis has both adaptive and maladaptive functions depending on the context and extent of fibrosis. On one hand, myocardial fibrosis is a cardinal feature of virtually all forms of heart disease, including hypertension, myocardial infarction, and heart failure.[31, 35, 42] In this context, long-term fibrosis perturbs cardiac contractility, lusitropy, electrical activation and electrical repolarization, contributing importantly to disease.[30, 43] Yet, short-term fibrosis, for example post-MI, is considered an adaptive response.

The heart continuously adapts to physiological and disease-related stressors, leading to complex and highly orchestrated events that culminate in both short and long-term adaptive responses.[44, 45] In this regard, cardiac fibrosis is a pervasive adaptive response that arises following tissue damage.[31, 35] Consistent with this, we observed that after ventricular apical resection, I/R, or MI injury, extensively injured areas are repopulated by cardiac fibroblasts harboring a primary cilium. We observed similar abundance of ciliated fibroblasts localized adjacent to the zone of injury in samples from human hearts with ischemic cardiomyopathy.

Fibroblasts are one of the most abundant cell types in the heart, playing a fundamental role in ECM homeostasis and wound healing.[46] In the setting of disease-related stress, cardiac fibroblasts differentiate into myofibroblasts triggered by TGF-β1. These cells are specialized in ECM protein secretion and contribute to fibrogenesis.[35, 46] This process is characterized by the synthesis, secretion and degradation of the ECM network, including fibronectin, collagen types I and III, as well as increased matrix metalloproteinase activity.[47] Both the paracrine action of TGF-β1 in the heart and treatment of primary cultures of cardiac fibroblasts with exogenous TGF-β1 elicited increases in phosphorylation of SMAD3 and transcription of fibronectin and collagen type I and III genes. Down-regulation of SMAD2/3 signaling with specific chemical inhibitors or siRNA blunts the fibrotic response induced by TGF-β1 in fibroblast cultures.[36] Findings reported here reveal that the cardiac fibroblast primary cilium is a critical element in TGF-β1 responsiveness, SMAD3 activation, ECM biogenesis, and fibrosis.

Primary ciliary structural elements and signal transduction

PC1 is a protein localized to the endoplasmic reticulum and within primary cilia.[48] In the primary cilium cell membrane, PC1 interacts with several proteins through its carboxy-terminal coiled-coil domains to activate diverse signaling pathways.[49] In addition, PC1 harbors a large amino-terminal extracellular domain comprising several peptide motifs that facilitate interaction with the extracellular matrix to promote cell-cell interactions.[50] We have reported previously that PC1 governs L-type Ca^{2+} channel protein stability in cardiomyocytes.[51]

The axoneme of the primary cilium typically has a ring of nine outer microtubule triplets (“9+0”) that lacks dynein arms and radial spokes.[14, 40] Intraflagellar transport (IFT) along the cilium is crucial for their formation, maintenance, and function.[10] A number of IFT proteins, such as IFT88, and KIF3A, an essential subunit of the kinesin II motor protein, are required for cilium formation.[26] Indeed, downregulation of IFT proteins or KIF3A are sufficient to disrupt cilia structure.[25]

Earlier work has suggested a role for cilia in TGF-β1 signaling in the developing heart.[40] Given that cardiac fibroblasts are the cells involved in the deposition of ECM, we hypothesized that cilia and PC1 may have a crucial role in the development of cardiac fibrosis. During fibrosis, the autocrine and paracrine action of TGF-β1, via SMAD2, 3 and 4, elicit the expression and synthesis of proteins required for fibrosis, such as collagens type I and III, fibronectin and matrix metalloproteinases.[35, 42] We report here that structural ciliary proteins and PC1 are required for the expression of fibrotic markers mediated by TGF-β1 in cardiac fibroblasts. Similar findings were observed with collagen contractile function in cardiac fibroblasts and myofibroblasts. Our findings go on to show that depletion of ciliary structural proteins, as well as down-regulation of PC1, inhibited TGF-β1-induced SMAD3 phosphorylation.

PC1 regulates cardiac remodeling and scar architecture

Here, we unveil for first time the relevance of PC1 in cardiac fibrogenesis. Using a line of fibroblast-specific *Pkd1* knockout mice, we report that PC1 in activated fibroblasts

participates importantly in the post-MI remodeling process, including the hypertrophic growth response, scar area, and elicitation of soluble collagen. Interestingly, we did not detect differences in interstitial fibrosis or ECM protein levels in *Pkd1* knockouts post-MI. We interpret this to derive from the fact that the periostin promoter that drives Cre recombinase is activated after the MI[38]; as such, our model highlights events occurring after a period of time delay following the initial MI injury. Further work, including use of periostin-Cre mice as a control, will allow for corroboration of our findings. Nevertheless, this animal model has been studied previously, and it was reported that the postn-Cre allele does not compromise periostin expression[52] or elicit alterations in fibrotic responsiveness after MI.[38]

Consistent with our *in vivo* results, we found that PC1 is not required for the up-regulation of ECM proteins in cardiac myofibroblasts maintained in culture. However, silencing of PC1 in myofibroblasts altered the characteristic contractile phenotype of these cells. A potential explanation for these results includes alterations in focal adhesion proteins; it has been shown that FAK phosphorylation at tyrosine 397 is diminished in $Pkd1^{-/-}$ mutants.[33] Moreover, PC1 silencing in MDCK/E cells triggers increased expression of the integrin α2β1.[53] The contribution of PC1 to focal adhesion formation and dynamics in cardiac myofibroblasts warrants future investigation.

Limitations

A gene expressed exclusively in cardiac fibroblasts has not been described. As such, we employed the promoter of the gene coding for periostin to drive Cre recombinase. As noted earlier, the periostin gene is activated by myocardial stress; as such, *Pkd1* recombination occurred in myofibroblasts rather than in quiescent fibroblasts. Therefore, our findings highlight events occurring with some delay in the post-MI response. Future work will benefit from a model of cardiac-specific knockout of PC1 or silencing of PC1 within the primary cilium in quiescent cardiac fibroblasts.

Conclusions

Findings reported here reveal for the first time that the primary cilium is present in mouse, rat, and human hearts, specifically in cardiac fibroblasts but not in cardiomyocytes. In cardiac fibroblasts, structural ciliary proteins and PC1 participate critically in the response to myocardial injury and specifically, fibrogenesis. These organelles participate in TGF-β1-dependent signaling and elicitation of extracellular matrix elements. In so doing, our findings uncover novel fibrosis regulators and raise the prospect that this pathway may emerge as a target with therapeutic relevance.

Supplementary Material

Refer to Web version on PubMed Central for supplementary material.

ACKNOWLEDGMENTS

We thank Dr. Peter Igarashi for generously providing $Kif3A^{F/F}$ mice. We thank the Histo-Pathology Core at UT Southwestern Medical Center for skillful help and support.

SOURCES OF FUNDING

This work was supported by grants from Fondo Nacional de Desarrollo Científico y Tecnológico, FONDECYT (1140908, AC and 1140713, LG); Programa de Investigación Asociativa, PIA (ACT172066); Fondo de Financiamiento de Centros de Investigación en Áreas Prioritarias, FONDAP 15130011 (SL, AC, LG, GDA) from the Comisión Nacional de Investigación Científica y Tecnológica, CONICYT , Santiago, Chile; by the National Institutes of Health (HL-120732, JAH; HL-100401, JAH; HL-128215, JAH, R01 HL-135657, SJC), American Heart Association (14SFRN20510023, JAH; 14SFRN20670003; JAH), Fondation Leducq (11CVD04, JAH), and Cancer Prevention and Research Institute of Texas (RP110486P3, JAH); by the PEW Latin American Fellows Program in the Biomedical Science (00002991, AC). EV held a PhD fellowship award (CONICYT-PCHA/Doctorado Nacional 2015-n° 21150957). GGS was supported by a fellowship from the American Heart Association and the Theodore and Beulah Beasley Foundation (18POST34060230).

REFERENCES

1. Berbari NF, O'Connor AK, Haycraft CJ and Yoder BK. The primary cilium as a complex signaling center. Curr Biol. 2009;19:R526–535. DOI: 10.1016/j.cub.2009.05.025 [PubMed: 19602418]
2. Raghavan V and Weisz OA. Discerning the role of mechanosensors in regulating proximal tubule function. Am J Physiol Renal Physiol. 2016;310:F1–5. DOI:10.1152/ajprenal.00373.2015 [PubMed: 26662200]
3. Zhu D, Shi S, Wang H and Liao K. Growth arrest induces primary-cilium formation and sensitizes IGF-1-receptor signaling during differentiation induction of 3T3-L1 preadipocytes. J Cell Sci. 2009;122:2760–2768. DOI: 10.1242/jcs.046276 [PubMed: 19596798]
4. Gazea M, Tasouri E, Tolve M, Bosch V, Kabanova A, Gojak C, Kurtulmus B, Novikov O, Spatz J, Pereira G, Hubner W, Brodski C, Tucker KL and Blaess S. Primary cilia are critical for Sonic hedgehog-mediated dopaminergic neurogenesis in the embryonic midbrain. Dev Biol. 2016;409:55–71. DOI: 10.1016/j.ydbio.2015.10.033 [PubMed: 26542012]
5. Delling M, DeCaen PG, Doerner JF, Febvay S and Clapham DE. Primary cilia are specialized calcium signalling organelles. Nature. 2013;504:311–314. DOI: 10.1038/nature12833 [PubMed: 24336288]
6. Yuan X, Cao J, He X, Serra R, Qu J, Cao X and Yang S. Ciliary IFT80 balances canonical versus non-canonical hedgehog signalling for osteoblast differentiation. Nat Commun. 2016;7:11024 DOI: 10.1038/ncomms11024 [PubMed: 26996322]
7. Schneider L, Clement CA, Teilmann SC, Pazour GJ, Hoffmann EK, Satir P and Christensen ST. PDGFRalphaalpha signaling is regulated through the primary cilium in fibroblasts. Curr Biol. 2005;15:1861–1866. DOI: 10.1016/j.cub.2005.09.012 [PubMed: 16243034]
8. Han YM, Kang GM, Byun K, Ko HW, Kim J, Shin MS, Kim HK, Gil SY, Yu JH, Lee B and Kim MS. Leptin-promoted cilia assembly is critical for normal energy balance. J Clin Invest. 2014;124:2193–7. DOI: 10.1172/JCI69395 [PubMed: 24667636]
9. Wang Y, Davidow L, Arvanites AC, Blanchard J, Lam K, Xu K, Oza V, Yoo JW, Ng JM, Curran T, Rubin LL and McMahon AP. Glucocorticoid compounds modify smoothened localization and hedgehog pathway activity. Chem Biol. 2012;19:972–982. DOI: 10.1016/j.chembiol.2012.06.012 [PubMed: 22921064]
10. Pampliega O, Orhon I, Patel B, Sridhar S, Diaz-Carretero A, Beau I, Codogno P, Satir BH, Satir P and Cuervo AM. Functional interaction between autophagy and ciliogenesis. Nature. 2013;502:194–200. DOI: 10.1038/nature12639 [PubMed: 24089209]
11. Nauli SM, Jin X, AbouAlaiwi WA, El-Jouni W, Su X and Zhou J. Non-motile primary cilia as fluid shear stress mechanosensors. Methods Enzymol. 2013;525:1–20. DOI: 10.1016/B978-0-12-397944-5.00001-8 [PubMed: 23522462]
12. Brown JM and Witman GB. Cilia and Diseases. Bioscience. 2014;64:1126–1137. DOI: 10.1093/biosci/biu174 [PubMed: 25960570]
13. Mangos S, Lam PY, Zhao A, Liu Y, Mudumana S, Vasilyev A, Liu A and Drummond IA. The ADPKD genes pkd1a/b and pkd2 regulate extracellular matrix formation. Dis Model Mech. 2010;3:354–365. DOI: 10.1242/dmm.003194 [PubMed: 20335443]
14. Myklebust R, Engedal H, Saetersdal TS and Ulstein M. Primary 9 + 0 cilia in the embryonic and the adult human heart. Anat Embryol (Berl). 1977;151:127–139. [PubMed: 920963]

15. Lee SH and Somlo S. Cyst growth, polycystins, and primary cilia in autosomal dominant polycystic kidney disease. Kidney Res Clin Pract. 2014;33:73–78. DOI: 10.1016/j.krcp.2014.05.002 [PubMed: 26877954]
16. Toomer KA, Fulmer D, Guo L, Drohan A, Peterson N, Swanson P, Brooks B, Mukherjee R, Body S, Lipschutz JH, Wessels A and Norris RA. A role for primary cilia in aortic valve development and disease. Dev Dyn. 2017;246:625–634. DOI: 10.1002/dvdy.24524 [PubMed: 28556366]
17. Lee J, Oh DH, Park KC, Choi JE, Kwon JB, Lee J, Park K and Sul HJ. Increased Primary Cilia in Idiopathic Pulmonary Fibrosis. Mol Cells. 2018;41:224–233. DOI: 10.14348/molcells.2018.2307 [PubMed: 29477141]
18. Rash JE, Shay JW and Biesele JJ. Cilia in cardiac differentiation. J Ultrastruct Res. 1969;29:470–484. [PubMed: 5365371]
19. Diguet N, Le Garrec JF, Lucchesi T and Meilhac SM. Imaging and analyzing primary cilia in cardiac cells. Methods Cell Biol. 2015;127:55–73. DOI: 10.1016/bs.mcb.2015.01.008 [PubMed: 25837386]
20. Bystrevskaya VB, Lichkun VV, Krushinsky AV and Smirnov VN. Centriole modification in human aortic endothelial cells. J Struct Biol. 1992;109:1–12. [PubMed: 1286005]
21. Arikawa K and Williams DS. Acetylated alpha-tubulin in the connecting cilium of developing rat photoreceptors. Invest Ophthalmol Vis Sci. 1993;34:2145–2149. DOI: 10.1016/bs.mcb.2015.01.008 [PubMed: 8491566]
22. Parker AK, Le MM, Smith TS, Hoang-Minh LB, Atkinson EW, Ugartemendia G, Semple-Rowland S, Coleman JE and Sarkisian MR. Neonatal seizures induced by pentylenetetrazol or kainic acid disrupt primary cilia growth on developing mouse cortical neurons. Exp Neurol. 2016;282:119–127. DOI: 10.1016/j.expneurol.2016.05.015 [PubMed: 27181411]
23. Wainwright EN, Svingen T, Ng ET, Wicking C and Koopman P. Primary cilia function regulates the length of the embryonic trunk axis and urogenital field in mice. Dev Biol. 2014;395:342–354. DOI: 10.1016/j.ydbio.2014.08.037 [PubMed: 25224227]
24. Lin F, Hiesberger T, Cordes K, Sinclair AM, Goldstein LS, Somlo S and Igarashi P. Kidney-specific inactivation of the KIF3A subunit of kinesin-II inhibits renal ciliogenesis and produces polycystic kidney disease. Proc Natl Acad Sci U S A. 2003;100:5286–5291. DOI: 10.1073/pnas.0836980100 [PubMed: 12672950]
25. Temiyasathit S, Tang WJ, Leucht P, Anderson CT, Monica SD, Castillo AB, Helms JA, Stearns T and Jacobs CR. Mechanosensing by the primary cilium: deletion of Kif3A reduces bone formation due to loading. PLoS One. 2012;7:e33368 DOI: 10.1371/journal.pone.0033368 [PubMed: 22428034]
26. Kim S and Dynlacht BD. Assembling a primary cilium. Curr Opin Cell Biol. 2013;25:506–511. DOI: 10.1016/j.ceb.2013.04.011 [PubMed: 23747070]
27. Porrello ER, Mahmoud AI, Simpson E, Hill JA, Richardson JA, Olson EN and Sadek HA. Transient regenerative potential of the neonatal mouse heart. Science. 2011;331:1078–1080. DOI: 10.1126/science.1200708 [PubMed: 21350179]
28. Clement CA, Ajbro KD, Koefoed K, Vestergaard ML, Veland IR, Henriques de Jesus MP, Pedersen LB, Benmerah A, Andersen CY, Larsen LA and Christensen ST. TGF-beta signaling is associated with endocytosis at the pocket region of the primary cilium. Cell Rep. 2013;3:1806–1814. DOI: 10.1016/j.celrep.2013.05.020 [PubMed: 23746451]
29. Evans RA, Tian YC, Steadman R and Phillips AO. TGF-beta1-mediated fibroblast-myofibroblast terminal differentiation-the role of Smad proteins. Exp Cell Res. 2003;282:90–100. [PubMed: 12531695]
30. Good Euler G. and bad sides of TGFbeta-signaling in myocardial infarction. Front Physiol. 2015;6:66 DOI: 10.3389/fphys.2015.00066 [PubMed: 25788886]
31. Kong P, Christia P and Frangogiannis NG. The pathogenesis of cardiac fibrosis. Cell Mol Life Sci. 2014;71:549–574. DOI: 10.1007/s00018-013-1349-6 [PubMed: 23649149]
32. Castelli M, De Pascalis C, Distefano G, Ducano N, Oldani A, Lanzetti L and Boletta A. Regulation of the microtubular cytoskeleton by Polycystin-1 favors focal adhesions turnover to modulate cell adhesion and migration. BMC Cell Biol. 2015;16:15 DOI: 10.1186/s12860-015-0059-3 [PubMed: 25947155]

33. Nigro EA, Castelli M and Boletta A. Role of the Polycystins in Cell Migration, Polarity, and Tissue Morphogenesis. Cells. 2015;4:687–705. DOI: 10.3390/cells4040687 [PubMed: 26529018]
34. Rothenberg KE, Scott DW, Christoforou N and Hoffman BD. Vinculin Force-Sensitive Dynamics at Focal Adhesions Enable Effective Directed Cell Migration. Biophys J. 2018;114:1680–1694. DOI: 10.1016/j.bpj.2018.02.019 [PubMed: 29642037]
35. Rockey DC, Bell PD and Hill JA. Fibrosis--A Common Pathway to Organ Injury and Failure. N Engl J Med. 2015;373:396 DOI:10.1056/NEJMra1300575
36. Roubille F, Busseuil D, Merlet N, Kritikou EA, Rheaume E and Tardif JC. Investigational drugs targeting cardiac fibrosis. Expert Rev Cardiovasc Ther. 2014;12:111–125. DOI: 10.1586/14779072.2013.839942 [PubMed: 24218990]
37. Luo N, Conwell MD, Chen X, Kettenhofen CI, Westlake CJ, Cantor LB, Wells CD, Weinreb RN, Corson TW, Spandau DF, Joos KM, Iomini C, Obukhov AG and Sun Y. Primary cilia signaling mediates intraocular pressure sensation. Proc Natl Acad Sci U S A. 2014;111:12871–12876. DOI: 10.1073/pnas.1323292111 [PubMed: 25143588]
38. Chen G, Bracamonte-Baran W, Diny NL, Hou X, Talor MV, Fu K, Liu Y, Davogustto G, Vasquez H, Taegtmeyer H, Frazier OH, Waisman A, Conway SJ, Wan F and Cihakova D. Sca-1(+) cardiac fibroblasts promote development of heart failure. Eur J Immunol. 2018;48:1522–1538. DOI: 10.1002/eji.201847583 [PubMed: 29953616]
39. Engelmann T Cils vibratils, in Richet, C. Dictionnaire de physiologie. 1898;785.
40. Koefoed K, Veland IR, Pedersen LB, Larsen LA and Christensen ST. Cilia and coordination of signaling networks during heart development. Organogenesis. 2014;10:108–125. DOI: 10.4161/org.27483 [PubMed: 24345806]
41. Li Y, Klena NT, Gabriel GC, Liu X, Kim AJ, Lemke K, Chen Y, Chatterjee B, Devine W, Damerla RR, Chang C, Yagi H, San Agustin JT, Thahir M, Anderton S, Lawhead C, Vescovi A, Pratt H, Morgan J, Haynes L, Smith CL, Eppig JT, Reinholdt L, Francis R, Leatherbury L, Ganapathiraju MK, Tobita K, Pazour GJ and Lo CW. Global genetic analysis in mice unveils central role for cilia in congenital heart disease. Nature. 2015;521:520–524. DOI: 10.1038/nature14269 [PubMed: 25807483]
42. Leask A Getting to the heart of the matter: new insights into cardiac fibrosis. Circ Res. 2015;116:1269–1276. DOI: 10.1161/CIRCRESAHA.116.305381 [PubMed: 25814687]
43. Dobaczewski M, de Haan JJ and Frangogiannis NG. The extracellular matrix modulates fibroblast phenotype and function in the infarcted myocardium. J Cardiovasc Transl Res. 2012;5:837–847. DOI: 10.1007/s12265-012-9406-3 [PubMed: 22956156]
44. Hill JA and Olson EN. Cardiac plasticity. N Engl J Med. 2008;358:1370–1380. DOI: 10.1056/NEJMra072139 [PubMed: 18367740]
45. Levitt Katz L, Gidding SS, Bacha F, Hirst K, McKay S, Pyle L, Lima JA and Group TS. Alterations in left ventricular, left atrial, and right ventricular structure and function to cardiovascular risk factors in adolescents with type 2 diabetes participating in the TODAY clinical trial. Pediatr Diabetes. 2015;16:39–47. DOI: 10.1111/pedi.12119 [PubMed: 24450390]
46. Takeda N, Manabe I, Uchino Y, Eguchi K, Matsumoto S, Nishimura S, Shindo T, Sano M, Otsu K, Snider P, Conway SJ and Nagai R. Cardiac fibroblasts are essential for the adaptive response of the murine heart to pressure overload. J Clin Invest. 2010;120:254–265. DOI: 10.1172/JCI40295 [PubMed: 20038803]
47. Rosenkranz S TGF-beta1 and angiotensin networking in cardiac remodeling. Cardiovasc Res. 2004;63:423–432. DOI: 10.1016/j.cardiores.2004.04.030 [PubMed: 15276467]
48. Chapin HC, Rajendran V and Caplan MJ. Polycystin-1 surface localization is stimulated by polycystin-2 and cleavage at the G protein-coupled receptor proteolytic site. Mol Biol Cell. 2010;21:4338–4348. DOI: 10.1091/mbc.E10-05-0407 [PubMed: 20980620]
49. Behn D, Bosk S, Hoffmeister H, Janshoff A, Witzgall R and Steinem C. Quantifying the interaction of the C-terminal regions of polycystin-2 and polycystin-1 attached to a lipid bilayer by means of QCM. Biophys Chem. 2010;150:47–53. DOI: 10.1016/j.bpc.2010.02.005 [PubMed: 20206434]

50. Malhas AN, Abuknesha RA and Price RG. Interaction of the leucine-rich repeats of polycystin-1 with extracellular matrix proteins: possible role in cell proliferation. J Am Soc Nephrol. 2002;13:19–26. [PubMed: 11752017]

51. Pedrozo Z, Criollo A, Battiprolu PK, Morales CR, Contreras-Ferrat A, Fernandez C, Jiang N, Luo X, Caplan MJ, Somlo S, Rothermel BA, Gillette TG, Lavandero S and Hill JA. Polycystin-1 Is a Cardiomyocyte Mechanosensor That Governs L-Type Ca2+ Channel Protein Stability. Circulation. 2015;131:2131–2142. DOI: 10.1161/CIRCULATIONAHA.114.013537 [PubMed: 25888683]

52. Masuoka M, Shiraishi H, Ohta S, Suzuki S, Arima K, Aoki S, Toda S, Inagaki N, Kurihara Y, Hayashida S, Takeuchi S, Koike K, Ono J, Noshiro H, Furue M, Conway SJ, Narisawa Y and Izuhara K. Periostin promotes chronic allergic inflammation in response to Th2 cytokines. J Clin Invest. 2012;122:2590–2600. DOI: 10.1172/JCI58978 [PubMed: 22684102]

53. Battini L, Fedorova E, Macip S, Li X, Wilson PD and Gusella GL. Stable knockdown of polycystin-1 confers integrin-alpha2beta1-mediated anoikis resistance. J Am Soc Nephrol. 2006;17:3049–3058. DOI: 10.1681/ASN.2006030234 [PubMed: 17005934]

CLINICAL PERSPECTIVE

WHAT IS NEW?

- We report increased abundance of cells harboring a primary cilium in areas of myocardium injured by disease-related stress.
- We go on to provide evidence that these cells are fibroblasts.
- Activation of TGF-β1/SMAD3 axis is regulated by the primary cilium (KIF3A) and PC1 in adult and neonatal cardiac fibroblasts.
- We have positioned PC1 as a protein key to cardiac fibrogenesis.
- Genetic inactivation of PC1 blunted TGF-β1-triggered fibrogenesis in fibroblasts prior to their differentiation into myofibroblasts.

WHAT ARE THE CLINICAL IMPLICATIONS?

- As myocardial fibrosis is a significant problem in a wide array of cardiovascular diseases, our identification of new regulators of cardiac fibrosis – PC1 and the primary cilium – points to previously unrecognized mechanisms that may emerge as therapeutic targets with clinical relevance.
- Given that these proteins are expressed in heart, our findings point to cardiomyocyte-autonomous mechanisms of fibrosis in patients with autosomal dominant polycystic kidney disease (ADPKD).

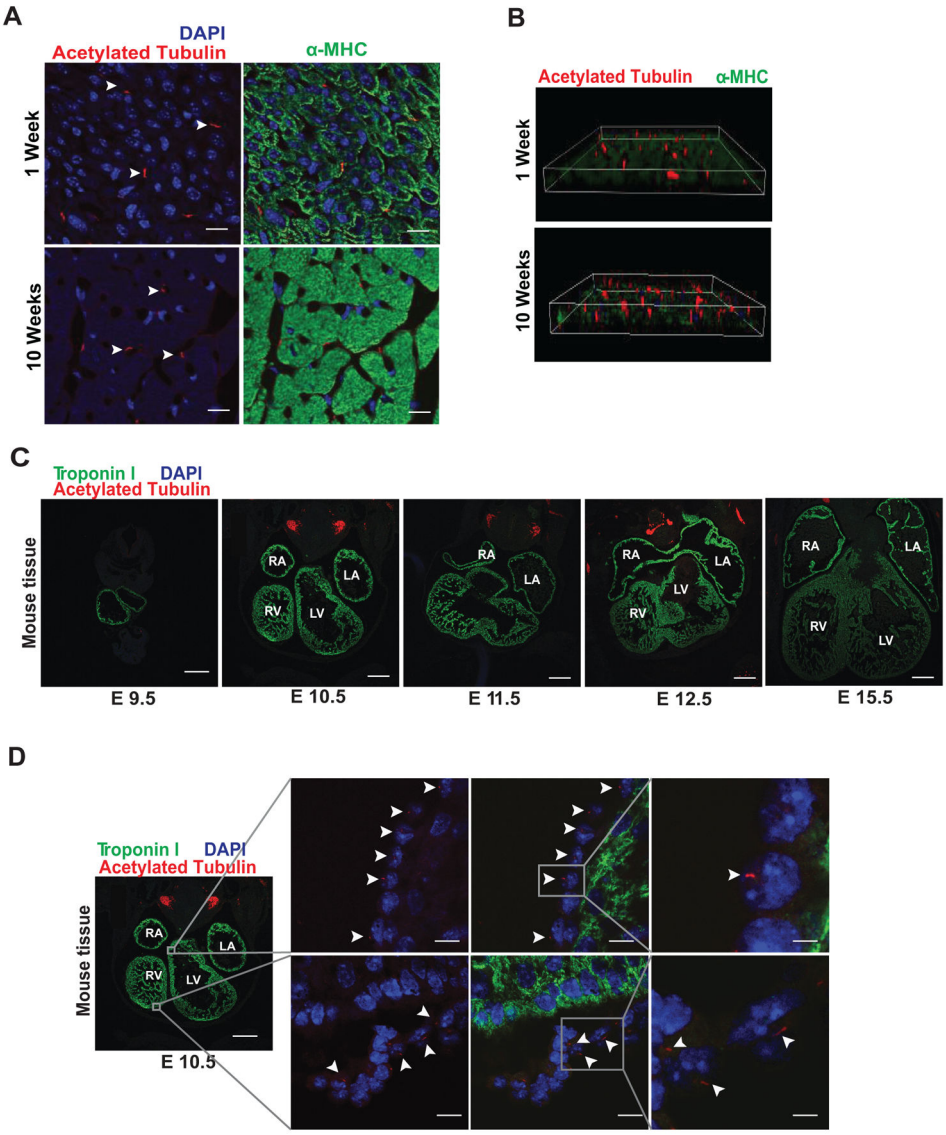

Figure 1. Primary cilia are present in the heart.

(**A**) Hearts were harvested from 1- and 10-week-old male, C57BL/6 mice. Hearts were embedded in paraffin, and tissue sections were evaluated by immunofluorescence staining for acetylated tubulin (red) and α-MHC (green), (scale bar: 20 μm). (**B**) 3D reconstruction images from (**A**). (**C** and **D**) Mouse embryos were harvested at embryonic day (E): E9.5, E10.5, E11.5, E12.5 and E15.5. Then, embryos were embedded in paraffin and whole-body slices analyzed by immunofluorescence staining for acetylated tubulin (red) and troponin I (green, marker for cardiomyocytes). Nuclei were stained with DAPI (blue) (100 μg/mL), and representative images were collected using a confocal microscope (n=3). White arrowheads highlight the presence of ciliated cells. Right (RA), left atrium (LA), and left (LV) and right ventricles (RV) are indicated (scale bars: 50 and 20 μm).

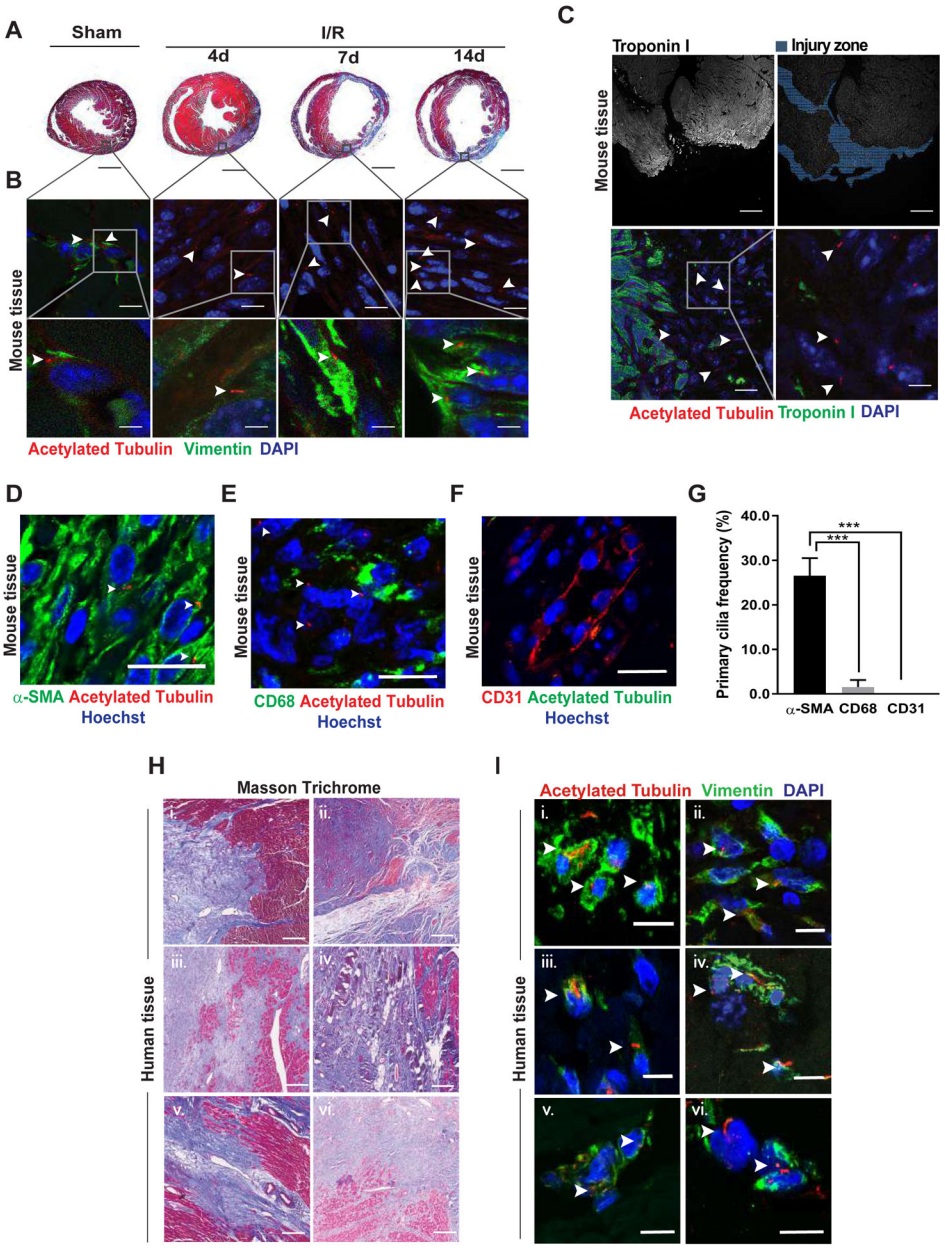

Figure 2. Ciliated cells accumulate in zones of injured myocardium.

(**A** and **B**) 10–12 week-old male, C57BL/6 mice were subjected to ischemia (45 min) (I). Hearts were harvested 4, 7, or 14 days later (reperfusion, R). Sham surgery was used as control. (**A**) Masson trichrome staining was performed in two-chamber sections to evaluate for changes in collagen deposition (scale bar: 1 mm). (**B**) Ciliated cells from heart samples from **(A)** were evaluated by acetylated tubulin immunostaining; vimentin was used as fibroblast marker. White arrowheads indicate the presence of cilia (scale bars: 20 and 5 μm). (**C**) 7 day-old C57BL/6 mice underwent apical resection surgery. Hearts were harvested 7 days post-resection, and the presence of ciliated cells was assessed by immunofluorescence for acetylated tubulin; troponin I was used as cardiomyocyte marker. (**D**-**F**) Myocardial infarction (MI) surgery was performed in 10–12 week-old male, C57BL/6 mice. (**D**) α-SMA

was used as a myofibroblast marker. (**E**) CD68 staining served as a macrophage marker, and (**F**) CD31 served as endothelial cell marker (scale bar: 20 μm). Hearts were harvested 7 days post-MI. The presence of cilia was evaluated in the scar area by immunofluorescence staining for acetylated tubulin. (**G**) Quantification of ciliated cells positive for α-SMA, CD68, and CD31 depicted in (**D-F**). Data are presented as mean percentage ± S.E.M., one-way ANOVA with Dunnet *post-hoc* test, ***$p \leq 0.001$ vs α-SMA (n=3–4). (**H** and **I**) Human heart tissue samples from 6 patients with stage IV heart failure were obtained at the time of cardiac transplantation and then subjected to (**H**) Masson trichrome staining to evaluate fibrosis (scale bar: 800 μm) and (**I**) immunofluorescence to evaluate ciliated cells (acetylated tubulin); vimentin served as a fibroblast marker (scale bar: 20 μm). For all images, nuclei were stained with either DAPI or Hoechst (100 μg/mL and 1 μg/mL, respectively), and images representative of 3–4 different animals are depicted. Images were obtained using a confocal microscope. White arrowheads highlight the presence of ciliated cells.

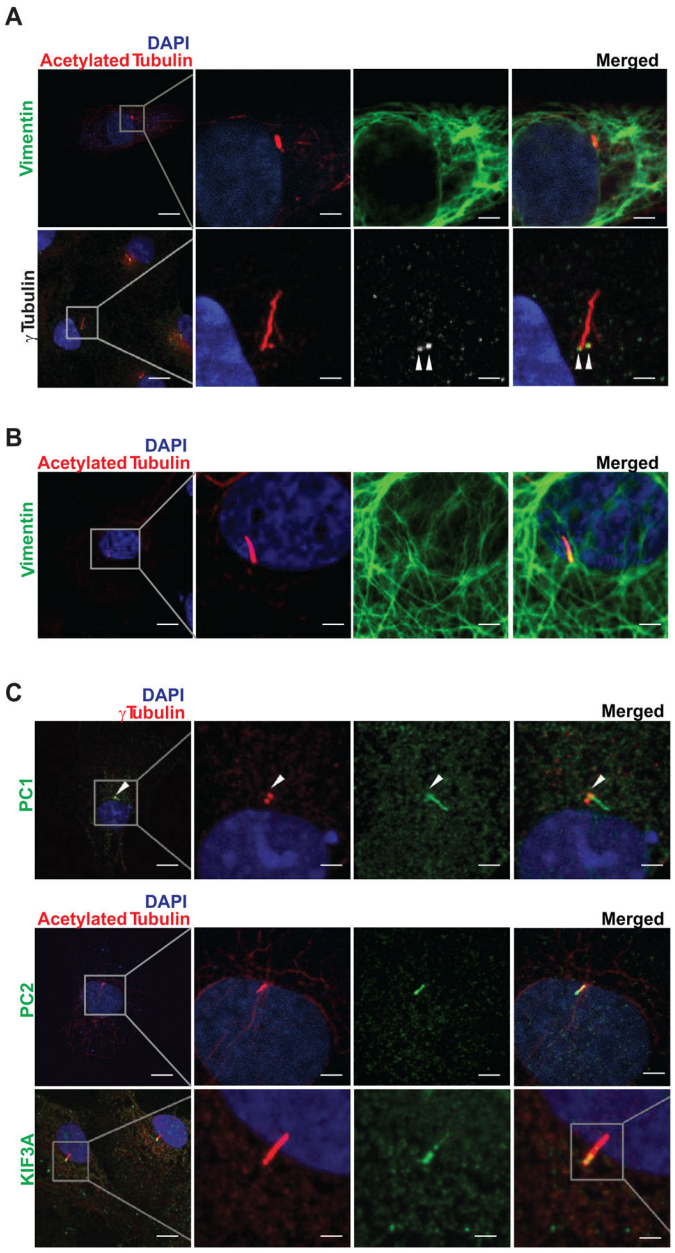

Figure 3. Primary cilia, PC1, PC2, and KIF3A are present in cardiac fibroblasts.

Primary cultures of (**A**) neonatal and (**B**) adult rat cardiac fibroblasts (NRCF and ARCF, respectively) were prepared, and immunofluorescence assays were performed to evaluate (**A-C**) vimentin, acetylated tubulin, γ-tubulin, PC1, PC2, and KIF3A. Nuclei were stained with DAPI (100 μg/mL). Representative images from 3 different cultures were obtained using a confocal microscope (scale bars: 20 and 5 μm). White arrowheads highlight the base of the cilium where γ-tubulin immunofluorescence was detected.

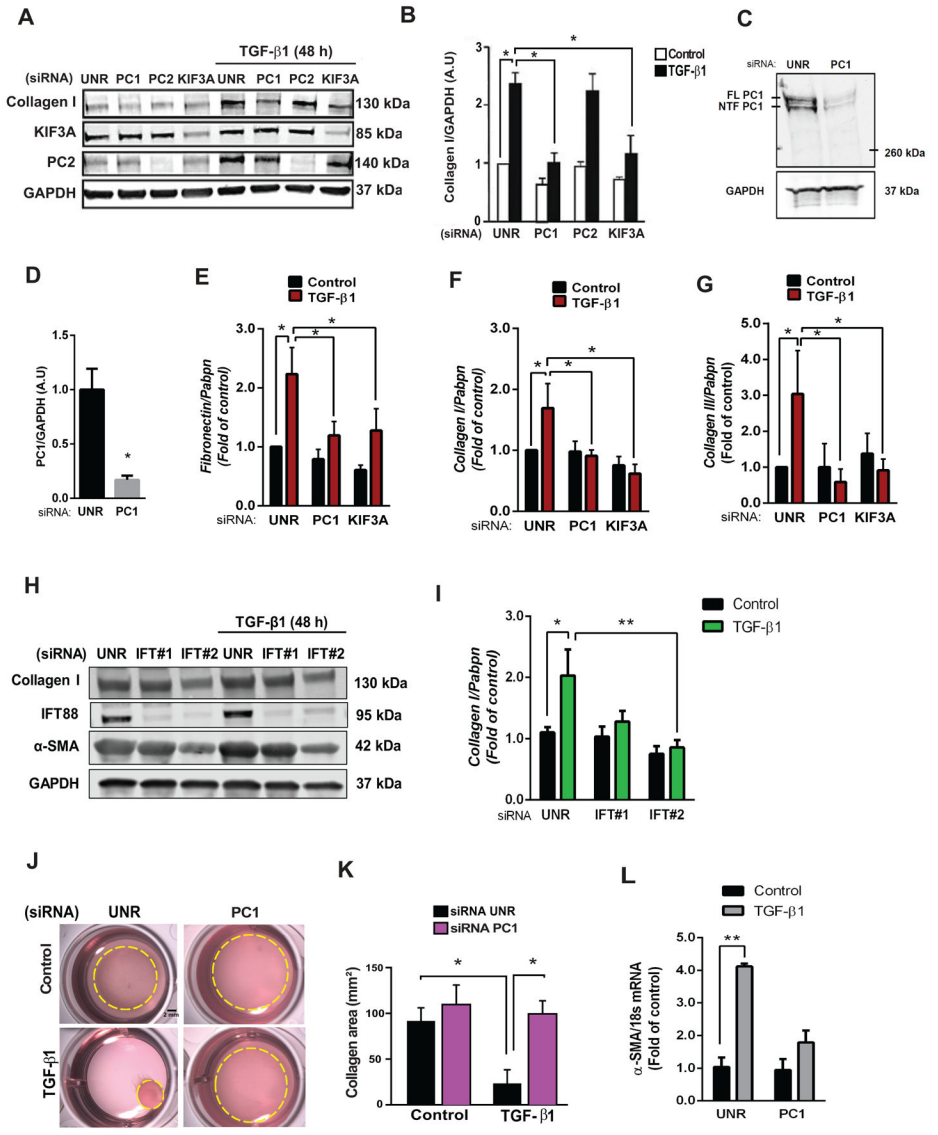

Figure 4. Cilia and PC1 are required for TGF-β1-induced cardiac fibrosis.

(**A** and **B**) Cultures of NRCF were prepared, and depletion of PC1, PC2 and KIF3A was accomplished using specific siRNAs versus control (unrelated siRNA, UNR). Cells were then treated with 10 ng/mL TGF-β1 for 48 h and total protein extracts or RNA were isolated. (**A**) Collagen type I, KIF3A, and PC2 were evaluated by Western blotting. GAPDH was used as loading control. Gels representative of three independent experiments are depicted. Gels shown in (**A**) were quantified (**B**). Data are represented as mean ± S.E.M. Two-way ANOVA, followed by Tukey's *post-hoc* test. *$p < 0.05$, n=3 independent cell cultures. (**C** and **D**) Knockdown of PC1 in ARCF. (**C**) PC1 protein levels after knockdown with siRNA (36 h) were evaluated by Western blotting: FL: full length PC1; NTF: N-terminal PC1. (**D**) Average densitometry from 3 independent cultures. Data are shown as mean ± S.E.M. Unpaired Student's *t*-test, *$p < 0.05$ vs UNR. **(E-G)** Transcript levels of (**E**) *fibronectin*, (**F**) *collagen I* and (**G**) *collagen III* were analyzed by quantitative RT-PCR, and *Pabpn* was used as housekeeping gene. Results are normalized to 1, and data are depicted as mean ± S.E.M.

Two-way ANOVA followed by Tukey's *post-hoc* test. *$p < 0.05$ (n=5–7). (**H** and **I**) Cultures of ARCF were prepared, and depletion of IFT88 with two sequence-independent siRNAs was performed. Cells were then treated with 10 ng/mL TGF-β1 for 48 h and total protein extracts were isolated. (**H**) Collagen type I, α-SMA and IFT88 levels were evaluated by Western blotting. (**I**) GAPDH was used as loading control for quantifications. Data are presented as mean ± S.E.M., Two-way ANOVA, followed by Tukey's *post-hoc* test, *$p < 0.05$; **$p < 0.01$ (n=3 independent cultures). Representative images (**J**) and quantification (**K**) of contraction of collagen matrices seeded with NRCF under control conditions (UNR) or following PC1 knockdown with or without TGF-β1 (48 h). Collagen area represents mean ± S.E.M. Two-way ANOVA, followed by Tukey's *post-hoc* test, *$p < 0.05$, n=3 independent cultures (Scale bar 2 mm). (**L**) Transcript levels of α-*SMA* were analyzed by quantitative RT-PCR, and *18s* was used as housekeeping gene. Results are normalized to 1, and data are depicted as mean ± S.E.M. Two-way ANOVA followed by Tukey's *post-hoc* test. *$p < 0.05$ (n=5–7)

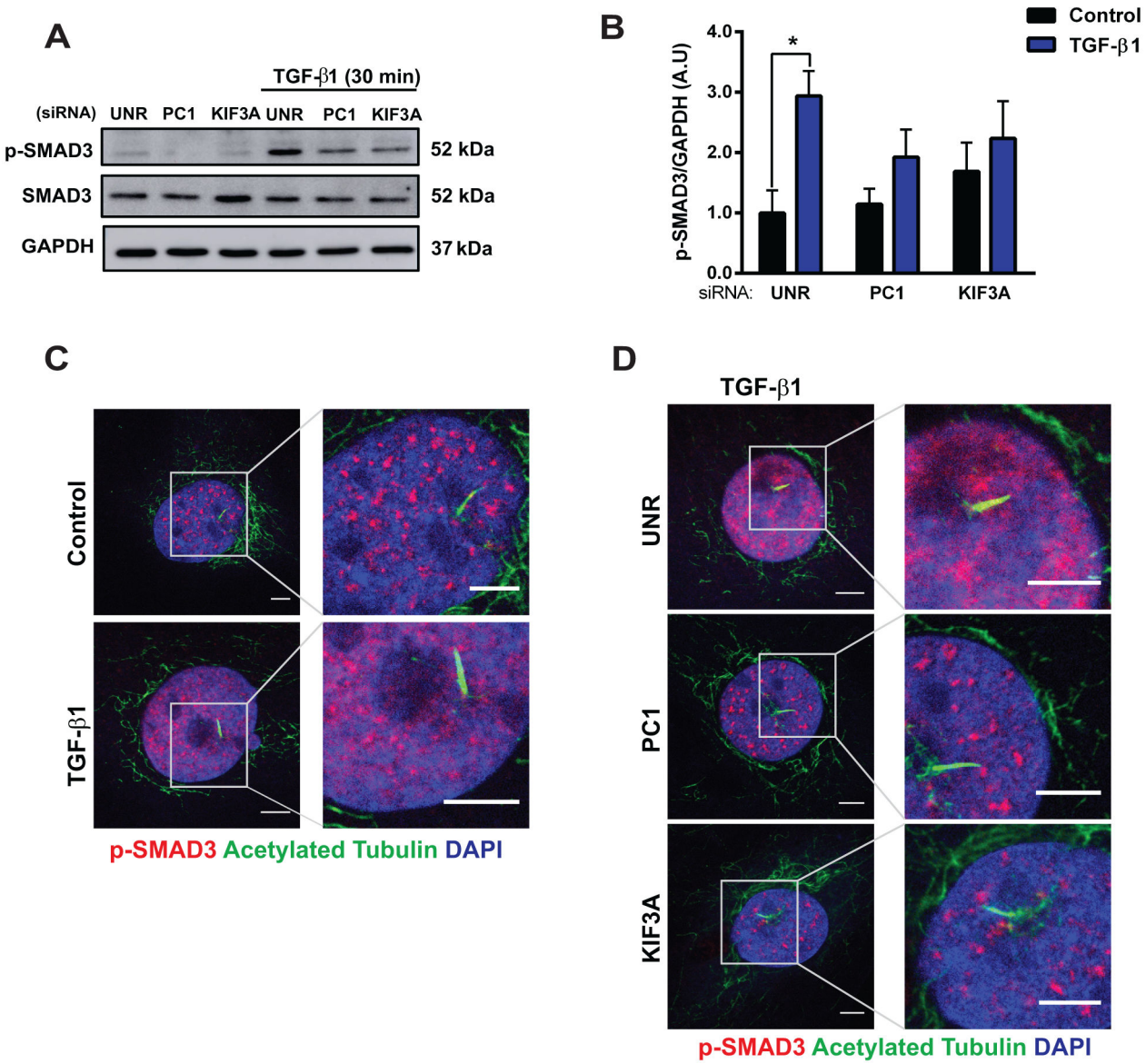

Figure 5. Cilia and PC1 are required for TGF-β1-triggered SMAD3 signaling.

Cultures of NRCF (**A** and **B**) and ARCF (**C** and **D**) were prepared and treated with 10 ng/mL TGF-β1 for 30 min in cells previously subjected to siRNA-mediated downregulation of PC1 or KIF3A. (**A** and **B**) Protein extracts were isolated, and p-SMAD3 and SMAD3 were evaluated by Western blotting. GAPDH was used as loading control. Gels were quantified, and values are depicted in (**B**). Data are mean ± S.E.M., two-way ANOVA, followed by Tukey's *post-hoc* test. *$p < 0.05$ (n=4 independent cultures). Immunofluorescence for acetylated tubulin (green) and p-SMAD3 (red) in **(C)** cultures of ARCF treated with or without TGF-β1 for 30 min and (**D**) cultures of ARCF depleted of PC1 or KIF3A using specific siRNAs. Cells were then treated with 10 ng/mL TGF-β1 for 30 min (n=3–4 independent cultures). Nuclei were stained with DAPI (100 μg/mL). Representative images were obtained using a confocal microscope (scale bar: 5 μm).

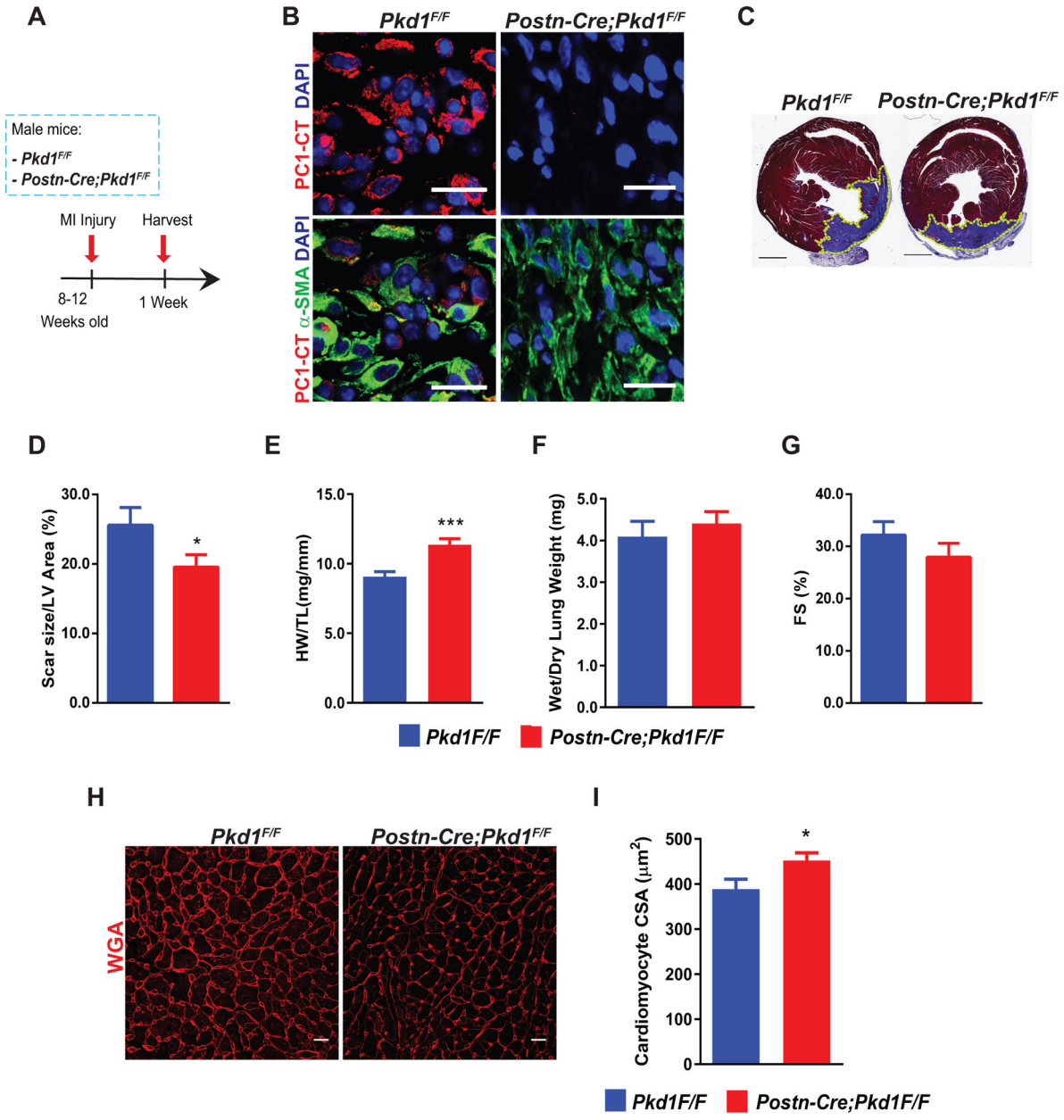

Figure 6. Fibroblast-specific PC1 inactivation enhances pathological cardiac remodeling following myocardial infarction (MI).

(**A**) MI surgery was performed in 8–12 week-old male mice of the following genotypes: *Pkd1*$^{F/F}$ and *Postn-Cre; Pkd1*$^{F/F}$. Hearts were harvested 1 week post-surgery. (**B**) Immunofluorescence from the scar zone to evaluate PC1 down-regulation in activated fibroblasts with PC1 C-terminal antibody (PC1-CT) and α-SMA as a marker of activated fibroblasts (scale bar: 20 μm). Nuclei were stained with DAPI (100 μg/mL), and images representative of 4 animals per group are depicted. Images were obtained using a confocal microscope. (**C**) Masson trichrome staining was performed to evaluate fibrosis and scar size. Representative images (n=12 animals per group) were obtained using a slide scanner (scale bar: 1 mm). (**D**) Scar size quantification. Data are shown as mean ± S.E.M., unpaired

Student's *t*-test with Welch's correction, n=12 animals per group. *$p < 0.05$. Morphometric analyses were performed after MI. (**E**) Heart weight/tibia length (HW/TL) and (**F**) wet/dry lung weight. Data are shown as mean ± S.E.M., unpaired Student's *t*-test with Welch's correction, n=19–21 animals per group. ***$p < 0.001$. (**G**) Ventricular contractile function was evaluated by transthoracic echocardiography. Fractional shortening (FS). Data are shown as mean ± S.E.M., unpaired Student's *t*-test with Welch's correction, n=19–22 animals per group. *$p < 0.05$. (**H** and **I**) Evaluation of cardiomyocyte cross-sectional area (CSA) after MI by wheat germ agglutinin (WGA) staining. (**H**) Representative images of WGA staining. Images were obtained with a confocal microscope (scale bar 20 μm). (**I**) Quantification of data depicted in (**H**). Data are shown as mean ± S.E.M., unpaired Student's t-test with Welch's correction, n=10–11 animals per group. *$p < 0.05$.

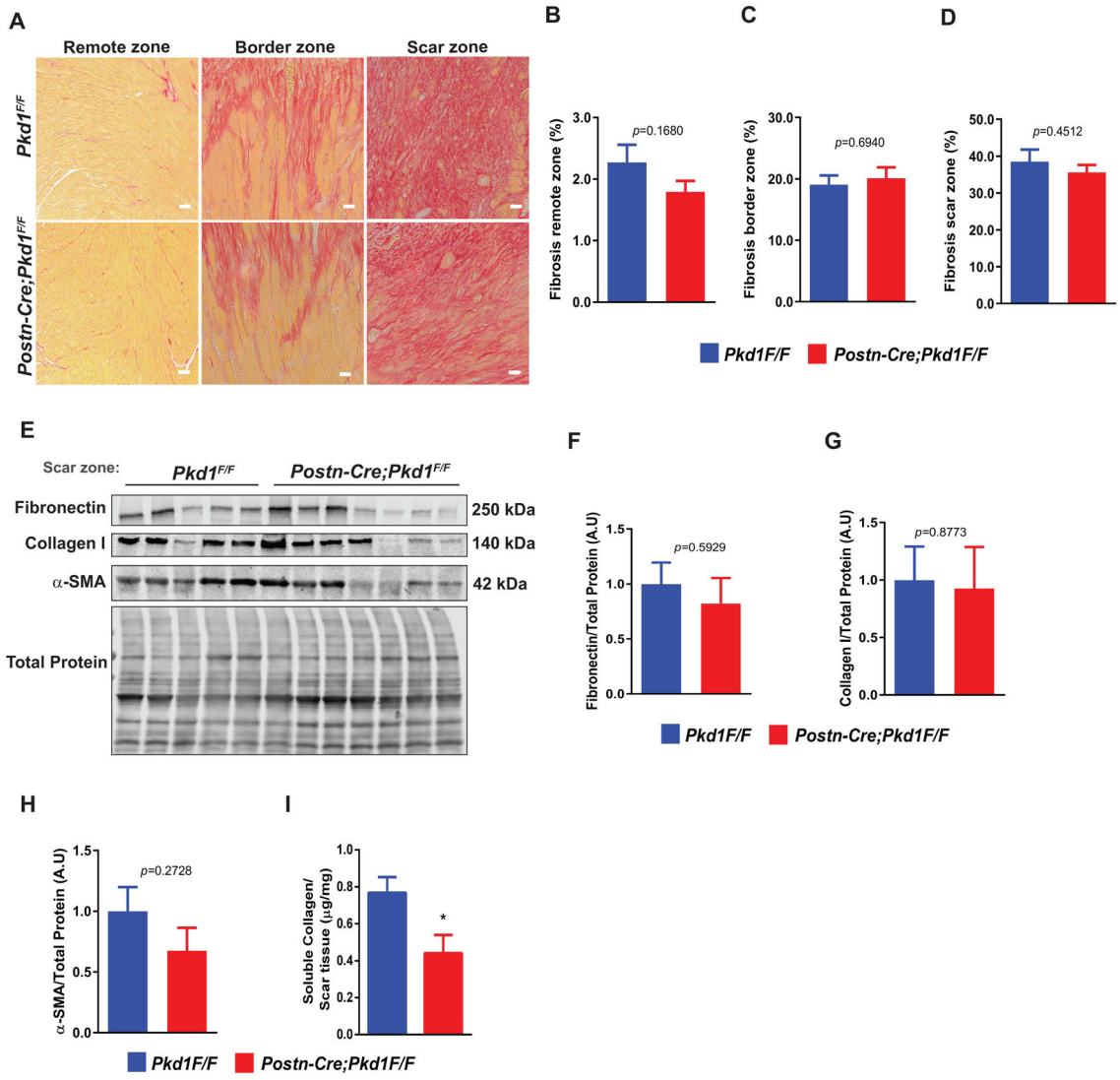

Figure 7. Alterations in scar composition in fibroblast-specific PC1 knockouts post-MI.

(**A-H**) MI surgery was performed in 8–12 week-old male mice of the following genotypes: *Pkd1*$^{F/F}$ and *Postn-Cre; Pkd1*$^{F/F}$. Hearts were harvested 7 days post-surgery. (**A**) Picrosirius red staining was performed to evaluate collagen deposition in the remote, border and scar zones (scale bar: 20 μm). (**B-D**) Quantification of fibrosis area depicted in (**A**). (**E-H**) Protein extracts were isolated from the scar, and protein levels of fibronectin, collagen I, and α-SMA were evaluated by Western blotting. Total protein was used as loading control. Gels were quantified, and values are depicted in (**F-H**), respectively. (**I**) Sircol assay was performed from scar tissue to measure soluble collagen levels. Data are shown as mean ± S.E.M., unpaired Student's t-test with Welch's correction, n= 8–10 animals per group. * $p < 0.05$.

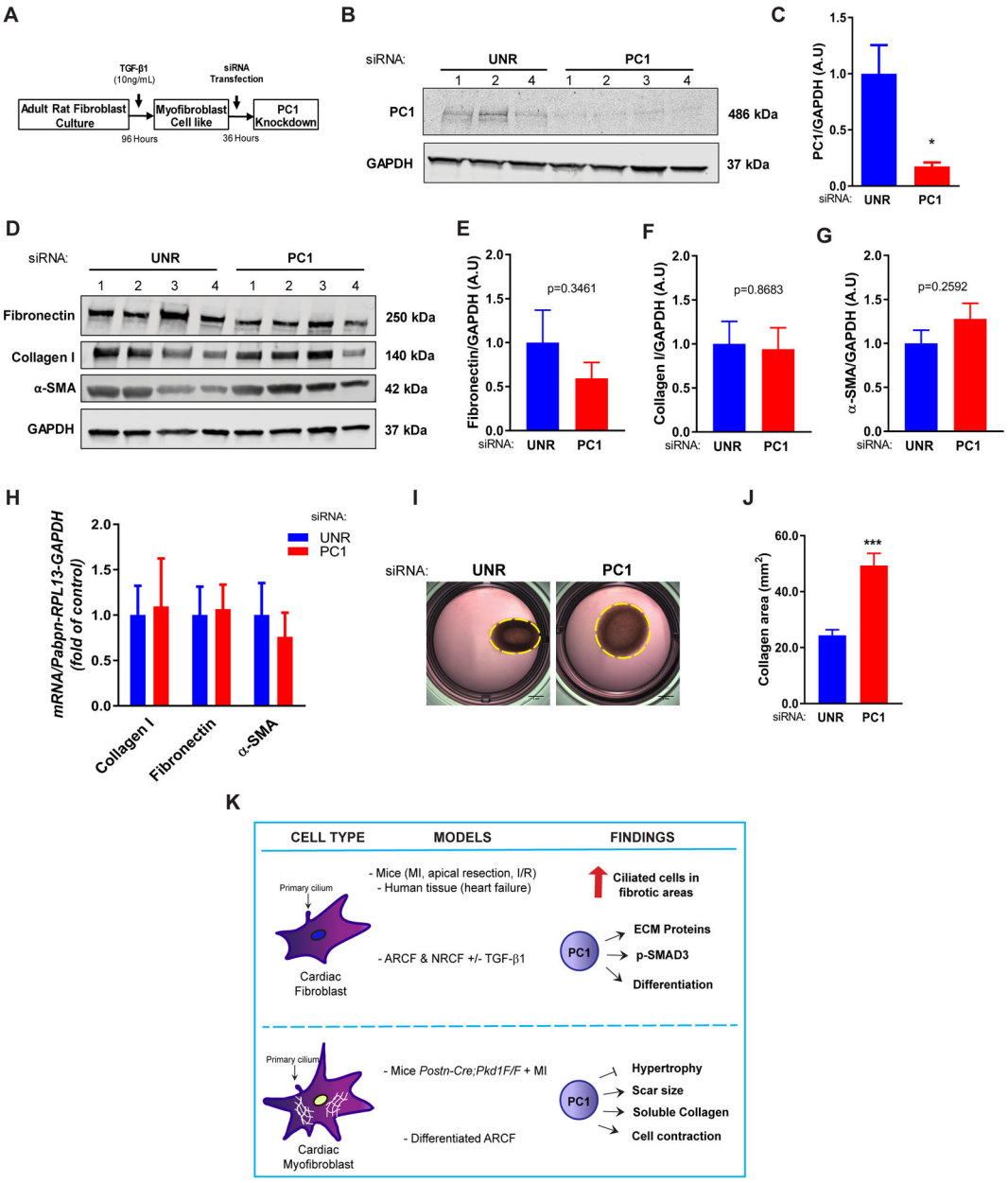

Figure 8. PC1 is required for myofibroblast contractile function.

(**A-J**) ARCF were isolated and differentiated with TGF-β1 (10 ng/mL, 96 h). After that, depletion of PC1 versus control (unrelated, UNR) was performed using specific siRNAs. Total protein extracts were isolated. (**B** and **C**) PC1 knockdown was evaluated by Western blotting. GAPDH was used as loading control. Gels depicted are representative of 3–4 different cultures. Gels shown in (**B**) were quantified (**C**). (**D-G**) Total protein extracts were isolated, and protein levels of fibronectin, collagen I, and α-SMA were evaluated by Western blotting. GAPDH was used as loading control. Gels depicted are representative of 4 independent cultures. Gels shown in (**F**) were quantified, and values are depicted in (**E-G**), respectively. (**H**) RNA isolation from total extracts was performed to evaluate gene expression of *collagen I, fibronectin, collagen III*, and *α-SMA* using quantitative RT-PCR.

Pabpn, RPL13 and *GAPDH* were used as housekeeping genes. Data are shown as mean ± S.E.M., unpaired Student's *t*-test, n = 7 independent cultures. **p* < 0.05. (**I** and **J**) Contraction of collagen matrices seeded with differentiated ARCF under control conditions (UNR) or following PC1 knockdown. (**I**) Representative images and collagen area quantification in (**J**). Data are shown as mean ± S.E.M., unpaired Student's *t*-test, n = 6, from 2 independent cultures. *** *p* < 0.001 (**K**) Graphical summary of our principal findings.